

# Spin Waves and Skyrmions in Magneto-Ferroelectric Superlattices: Theory and Simulation <sup>†</sup>

Hung T. Diep <sup>1,\*</sup> and Ildus F. Sharafullin <sup>2,‡</sup>

<sup>1</sup> Laboratoire de Physique Théorique et Modélisation, Université de Cergy-Pontoise, CNRS, UMR 8089, 2 Avenue Adolphe Chauvin, 95302 Cergy-Pontoise CEDEX, France

<sup>2</sup> Bashkir State University, 32, Validy Str., 450076 Ufa, Russia; sharafullinif@yandex.ru

\* Correspondence: diep@u-cergy.fr

<sup>†</sup> Presented at the 5th International Electronic Conference on Entropy and Its Applications, 18–30 November 2019; Available online: <https://ecea-5.sciforum.net/>.

<sup>‡</sup> These authors contributed equally to this work.

Published: 17 November 2019



**Abstract:** We present in this paper the effects of Dzyaloshinskii–Moriya (DM) magnetoelectric coupling between ferroelectric and magnetic layers in a superlattice formed by alternate magnetic and ferroelectric films. Magnetic films are films of simple cubic lattice with Heisenberg spins interacting with each other via an exchange  $J$  and a DM interaction with the ferroelectric interface. Electrical polarizations of  $\pm 1$  are assigned at simple cubic lattice sites in the ferroelectric films. We determine the ground-state (GS) spin configuration in the magnetic film. In zero field, the GS is periodically non-collinear (helical structure) and in an applied field  $\mathbf{H}$  perpendicular to the layers, it shows the existence of skyrmions at the interface. Using the Green’s function method we study the spin waves (SW) excited in a monolayer and also in a bilayer sandwiched between ferroelectric films, in zero field. We show that the DM interaction strongly affects the long-wave length SW mode. We calculate also the magnetization at low temperatures. We use next Monte Carlo simulations to calculate various physical quantities at finite temperatures such as the critical temperature, the layer magnetization and the layer polarization, as functions of the magneto-electric DM coupling and the applied magnetic field. Phase transition to the disordered phase is studied.

**Keywords:** superlattice; magneto-ferroelectric coupling; spin waves; skyrmions; phase transition; Green’s function theory; Monte Carlo simulation

## 1. Introduction

The localized topological spin-textures “magnetic skyrmions” are of great interest nowadays due to their fundamental and practical importance [1–6]. Skyrmions hold great promise as a basis for future digital technologies [7–15]. Information flow in next-generation spintronic devices could be associated with metastable isolated skyrmions guided along magnetic stripes [14,16–18]. Skyrmions have been experimentally observed, created, and manipulated in a number of material systems, including magnetic materials [2,4,5,7,19–27], multiferroic materials [28], ferroelectric materials [29], and semiconductors [30]. Skyrmions have been recently observed in conducting and insulating helimagnets under an applied magnetic field [2,20]. Under an applied magnetic field, the spiral structure due to a Dzyaloshinskii–Moriya (DM) transforms into a skyrmion crystal [31].

Multiferroics and superlattices of multiferroics (for example, *PZT/LSMO* and *BTO/LSMO*) are attracting increasing interest and provoking much research activity driven by the profound physics of these materials, the coexistence and coupling of ferroelectric and magnetic orders. Enormous

attention was paid to studying the non-uniform states in magnetic/ferroelectric superlattices both theoretically [32] and experimentally [33–35].

Recently, magnetic/ferroelectric superlattices have attracted much of attention as magneto-electric (ME) materials [34,35]. Spin waves and skyrmions in “unfrustrated” magnetolectric superlattices with a Dzyaloshinskii–Moriya (DM) interface coupling have been studied [32].

The purpose of this paper is to show the main features of our results obtained for a magneto-ferroelectric superlattice where the interface coupling is a DM interaction. The effect of the frustration due to the competing next-nearest-neighbor (NNN) interaction is emphasized.

The paper is organized as follows. Section 2 is devoted to the description of our model and the determination of the ground-state spin configuration with and without applied magnetic field. Skyrmion crystal is shown with varying interface parameters. Section 3 shows the results for spin-wave spectrum obtained by the Green’s function method. Results of Monte Carlo simulations for the phase transition in the system is shown in Section 4. These results show that the skyrmion crystal is stable at finite temperatures below a transition temperature  $T_c$ . Concluding remarks are given in Section 5.

## 2. Model: Ground State

Consider a superlattice composed of alternate magnetic and ferroelectric films. Both have the structure of simple cubic lattice of the same lattice constant, for simplicity. The Hamiltonian of this multiferroic superlattice is expressed as:

$$\mathcal{H} = H_m + H_f + H_{mf} \quad (1)$$

where  $H_m$  and  $H_f$  are the Hamiltonians of the magnetic and ferroelectric subsystems, respectively,  $H_{mf}$  denotes Hamiltonian of magnetolectric interaction at the interface of two adjacent films. We are interested in the frustrated regime. Therefore we describe the Hamiltonian of the magnetic film with the Heisenberg spin model on a simple cubic lattice as follows:

$$H_m = - \sum_{i,j} J_{ij}^m \mathbf{S}_i \cdot \mathbf{S}_j - \sum_{i,k} J_{ik}^{2m} \mathbf{S}_i \cdot \mathbf{S}_k - \sum_i \mathbf{H} \cdot \mathbf{S}_i \quad (2)$$

where  $\mathbf{S}_i$  is the spin on the  $i$ -th site,  $\mathbf{H}$  the external magnetic field,  $J_{ij}^m$  the magnetic interaction between two spins at  $i$  and  $j$  sites. We shall take into account both the nearest neighbors (NN) interaction, denoted by  $J^m$ , and the next-nearest neighbor (NNN) interaction denoted by  $J^{2m}$ . We consider  $J^m > 0$  to be the same everywhere in the magnetic film. To introduce the frustration we shall consider  $J^{2m} < 0$ , namely antiferromagnetic interaction, the same everywhere. The external magnetic field  $\mathbf{H}$  is applied along the  $z$ -axis which is perpendicular to the plane of the layers. The interaction of the spins at the interface will be given below.

For the ferroelectric film, we suppose for simplicity that electric polarizations are Ising-like vectors of magnitude 1, pointing in the  $\pm z$  direction. The Hamiltonian is given by

$$H_f = - \sum_{i,j} J_{ij}^f \mathbf{P}_i \cdot \mathbf{P}_j - \sum_{i,k} J_{ik}^{2f} \mathbf{P}_i \cdot \mathbf{P}_k \quad (3)$$

where  $\mathbf{P}_i$  is the polarization on the  $i$ -th lattice site,  $J_{ij}^f$  the interaction parameter between polarizations at sites  $i$  and  $j$ . Similar to the magnetic subsystem we will take the same  $J_{ij}^f = J^f > 0$  for all NN pairs, and  $J_{ij} = J^{2f} < 0$  for NNN pairs.

Before introducing the DM interface interaction, let us emphasize that the bulk  $J_1 - J_2$  model on the simple cubic lattice has been studied with Heisenberg spins [36] and the Ising model [37] where  $J_1$  and  $J_2$  are both antiferromagnetic ( $< 0$ ). The critical value  $|J_2^c| = 0.25|J_1|$  above which the bipartite antiferromagnetic ordering changes into a frustrated ordering where a line is with spins up, and its neighboring lines are with spins down. In the case of  $J^m > 0$  (ferro), and  $J^{2m} < 0$ , it is easy to show

that the critical value where the ferromagnetic becomes antiferromagnetic is  $J_c^{2m} = -0.5J^m$ . Below this value, the antiferromagnetic ordering replaces the ferromagnetic ordering.

We know that the DM interaction is written as

$$H_{DM} = \mathbf{D}_{i,j} \cdot \mathbf{S}_i \times \mathbf{S}_j \tag{4}$$

where  $\mathbf{S}_i$  is the spin of the  $i$ -th magnetic ion, and  $\mathbf{D}_{i,j}$  is the Dzyaloshinskii–Moriya vector. The vector  $\mathbf{D}_{i,j}$  is proportional to the vector product  $\mathbf{R} \times \mathbf{r}_{i,j}$  of the vector  $\mathbf{R}$  which specifies the displacement of the ligand (for example, oxygen) and the unit vector  $\mathbf{r}_{i,j}$  along the axis connecting the magnetic ions  $i$  and  $j$  (see Figure 1). One then has

$$\begin{aligned} \mathbf{D}_{i,j} &= \mathbf{R} \times \mathbf{r}_{i,j} \\ \mathbf{D}_{j,i} &= \mathbf{R} \times \mathbf{r}_{j,i} = -\mathbf{D}_{i,j} \end{aligned} \tag{5}$$

We define thus

$$\mathbf{D}_{i,j} = D e_{i,j} \mathbf{z} \tag{6}$$

where  $D$  is a constant,  $\mathbf{z}$  the unit vector on the  $z$  axis, and  $e_{i,j} = -e_{j,i} = 1$ .

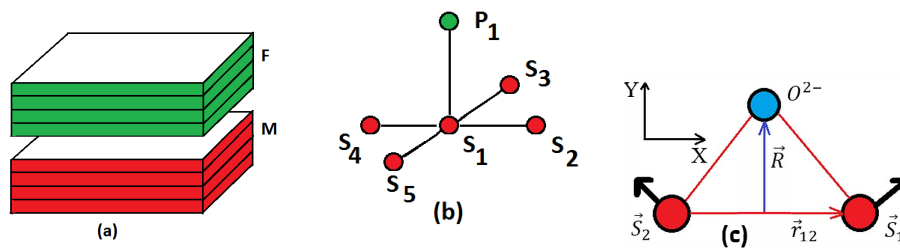


**Figure 1.** (a) Magneto-ferroelectric superlattice; (b) interfacial coupling between a polarization  $P$  with five spins in a Dzyaloshinskii–Moriya (DM) interaction; (c) positions of the spins in the  $xy$  plane and the position of non-magnetic ion oxygen, defining the DM vector (see text).

For the magnetoelectric interaction at the interface, we choose the interface Hamiltonian following reference [32]:

$$H_{mf} = \sum_{i,j,k} J_{i,j}^{mf} e_{i,j} \mathbf{P}_k \cdot [\mathbf{S}_i \times \mathbf{S}_j] \tag{7}$$

where  $\mathbf{P}_k$  is the polarization at the site  $k$  of the ferroelectric interface layer, while  $\mathbf{S}_i$  and  $\mathbf{S}_j$  belong to the interface magnetic layer. In this expression  $J_{i,j}^{mf} e_{i,j} \mathbf{P}_k$  plays the role of the DM vector perpendicular to the  $xy$  plane, given by Equation (6). When summing the neighboring pairs  $(i, j)$ , attention should be paid on the signs of  $e_{i,j}$  and  $\mathbf{S}_i \times \mathbf{S}_j$  (see example in reference [32]).

Hereafter, we suppose  $J_{i,j}^{mf} = J^{mf}$  independent of  $(i, j)$ .

Since  $\mathbf{P}_k$  is in the  $z$  direction, i. e. the DM vector is in the  $z$  direction, in the absence of an applied field the spins in the magnetic layers will lie in the  $xy$  plane to minimize the interface interaction energy, according to Equation (7).

From Equation (7), we see that the magnetoelectric interaction  $J^{mf}$  favors a canted (non collinear) spin structure. It competes with the exchange interactions  $J^m$  and  $J^{2m}$  of  $H_m$  which favor collinear (ferro and antiferro) spin configurations. In ferroelectric layers, there is just ferro- or antiferromagnetic ordering due to the Ising nature. Usually the magnetic or ferroelectric exchange interaction is the leading term in the Hamiltonian, so that in many situations the magnetoelectric effect is negligible. However, in nanofilms of superlattices the magnetoelectric interaction is crucial for the creation of non-collinear long-range spin order. It has been shown that Rashba spin-orbit coupling can lead to a

strong DM interaction at the interface [38,39], where the broken inversion symmetry at the interface can change the magnetic states.

Since the polarizations are along the  $z$  axis, the interface DM interaction is minimum when  $\mathbf{S}_i$  and  $\mathbf{S}_j$  lie in the  $xy$  interface plane and perpendicular to each other. However the collinear exchange interactions among the spins will compete with the DM perpendicular configuration. The resulting configuration is non-collinear. In the general case where a magnetic field is applied and there is also the frustration, we use the steepest descent method [31,32] to determine the ground state.

We show in Figure 2 an example where  $H = 0$  with no NNN interaction. The magnetic film has a single layer. The GS spin configurations have periodic structures. Several remarks are in order:

(i) Each spin has the same turning angle  $\theta$  with its NN in both  $x$  and  $y$  direction. The schematic zoom in Figure 2c shows that the spins on the same diagonal (spins 2 and 3, spins 4 and 5) are parallel. This explains the structures shown in Figure 2a,b;

(ii) The periodicity of the diagonal parallel lines depends on the value of  $\theta$  (comparing Figure 2a with Figure 2b). With a large size of  $N$ , the periodic conditions have no significant effects.

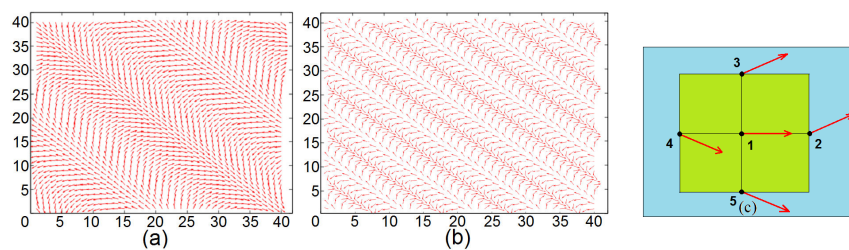


**Figure 2.** Ground-state (GS) spin configurations for (a)  $J^{mf} = -0.45$ ; (b)  $J^{mf} = -1.2$ , with  $H = 0$ ; (c) angles between nearest neighbors (NN) are schematically zoomed. See text for comments.

Let us show now an example with  $H \neq 0$  in Figure 3 with a frustration due to NNN interaction.

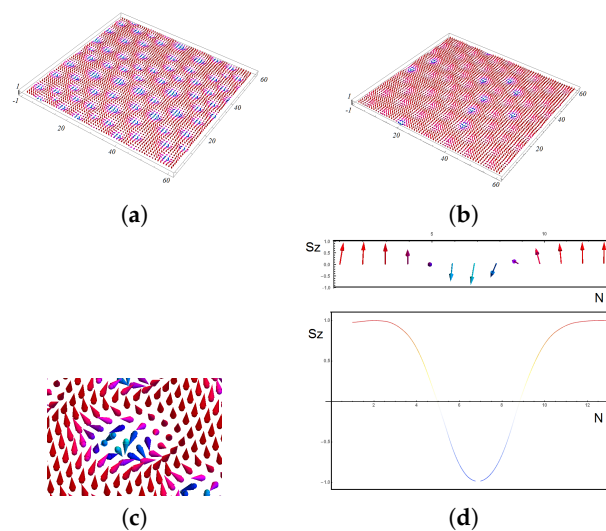


**Figure 3.** (a) Three-dimensional view of the GS configuration of the interface for moderate frustration  $J^{2m} = J^{2f} = -0.2$ ; (b) 3D view of the GS configuration of the second magnetic layers; (c) zoom of a skyrmion on the interface layer: Red denotes up spin, four spins with clear blue color are down spin, other colors correspond to spin orientations between the two. The skyrmion is of the Bloch type; (d)  $z$ -components of spins across the skyrmion shown in (c). Other parameters:  $J^m = J^f = 1$ ,  $J^{mf} = -1.25$  and  $H = 0.25$ .

At this field strength  $H = 0.25$ , if we increase the frustration, for example,  $J^{2m} = J^{2f} = -0.3$ , then the skyrmion structure is enhanced: we can observe a clear 3D skyrmion crystal structure not only in the interface layer but also in the interior layers (not shown).

Many other cases will be shown in a full paper.

### 3. Spin Waves

Here let us show theoretically spin-waves (SW) excited in the magnetic film in zero field, in some simple cases. The method we employ is the Green's function technique for non-collinear spin configurations which has been shown to be efficient for studying low- $T$  properties of quantum spin systems such as helimagnets [40] and systems with a DM interaction [41]. This technique is rather lengthy to describe here. The reader is referred to these papers for mathematical details.

Let us show here only the resulting spin-wave energy

$$E = \pm \sqrt{(A+B)(A-B)} \tag{8}$$

$$A = -J^m [8 \langle S^z \rangle \cos \theta (1+d) - 4 \langle S^z \rangle \gamma (\cos \theta + 1)] - 4D \sin \theta \langle S^z \rangle \gamma + 8D \sin \theta \langle S^z \rangle \tag{9}$$

$$B = 4J^m \langle S^z \rangle \gamma (\cos \theta - 1) - 4D \sin \theta \langle S^z \rangle \gamma \tag{10}$$

where the reduced anisotropy is  $d = K/J^m$  and  $\gamma = (\cos k_x a + \cos k_y a)/2$ ,  $k_x$  and  $k_y$  being the wave-vector components in the  $xy$  planes,  $a$  the lattice constant,  $\theta$  the angle between two NN spins given by  $\theta = \arctan(-\frac{2J^{mf}}{J^m})$ .

We show in Figure 4 the spin-wave energy  $E$  versus the wave vector  $k = k_x = k_y$ , for weak and strong values of the DM interaction strength  $D$ . For the weak value of  $\theta$  (Figure 4a), namely weak  $J^{mf}$ , the long-wave length mode energy ( $k \rightarrow 0$ ) is proportional to  $k^2$  as in ferromagnets, while for strong  $\theta$  (Figure 4b),  $E$  is proportional to  $k$  as in antiferromagnets. The effect of the DM interaction is thus very strong on the spin-wave behavior.

The case of a bilayer as well as the effects of other parameters on the spin-wave spectrum will be shown in the full paper.

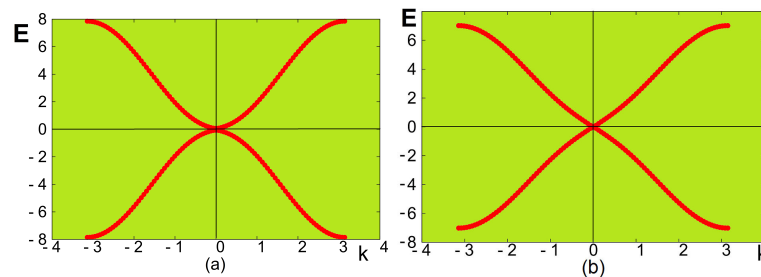


**Figure 4.** Spin-wave energy  $E(k)$  versus  $k$  ( $k \equiv k_x = k_z$ ) for (a)  $\theta = 0.3$  radian and (b)  $\theta = 1$  for a monolayer at  $T = 0$ . See text for comments.

### 4. Phase Transition

We have seen the skyrmion crystal in Figure 3 at  $T = 0$ . Shall this structure survive at finite  $T$ ? To answer this question we have performed Monte Carlo simulations using the Metropolis algorithm [42]. We have to define an order parameter for the skyrmion crystal. In complicated spin orderings such as spin glasses, we have to follow each individual spin during the time. If it is frozen then its time average is not zero. This is called Edwards–Anderson order parameter for spin glasses [43].

For the magnetic layers, the definition of an order parameter for a skyrmion crystal is not obvious. Taking advantage of the fact that we know the GS, we define the order parameter as the projection of

an actual spin configuration at a given  $T$  on its GS and we take the time average. This order parameter of layer  $n$  is thus defined as

$$M_m(n) = \frac{1}{N^2(t_a - t_0)} \sum_{i \in n} \left| \sum_{t=t_0}^{t_a} \mathbf{S}_i(T, t) \cdot \mathbf{S}_i^0(T=0) \right| \quad (11)$$

where  $\mathbf{S}_i(T, t)$  is the  $i$ -th spin at the time  $t$ , at temperature  $T$ , and  $\mathbf{S}_i(T=0)$  is its state in the GS. The order parameter  $M_m(n)$  is close to 1 at very low  $T$  where each spin is only weakly deviated from its state in the GS.  $M_m(n)$  is zero when every spin strongly fluctuates in the paramagnetic state.

For the ferroelectric layers, the order parameter  $M_f(n)$  of layer  $n$  is defined as the magnetization

$$M_f(n) = \frac{1}{N^2} \langle \left| \sum_{i \in n} P_i^z \right| \rangle \quad (12)$$

where  $\langle \dots \rangle$  denotes the time average. The total order parameters  $M_m$  and  $M_f$  are the sum of the layer order parameters, namely  $M_m = \sum_n M_m(n)$  and  $M_f = \sum_n M_f(n)$ .

In Figure 5 we show the magnetic energy and magnetic order parameter versus temperature in an external magnetic field, for various sets of NNN interaction. Note that the phase transition occurs at the energy curvature changes, namely at the maximum of the specific heat. The red curve in Figure 5a is for both sets ( $J^{2m} = J^{2f} = -0.4$ ), ( $J^{2m} = -0.4, J^{2f} = 0$ ). The change of curvature takes place at  $T_c^m \simeq 0.60$ . It means that the ferroelectric frustration does not affect the magnetic skyrmion transition at such a strong magnetic frustration ( $J^{2m} = -0.4$ ). For ( $J^{2m} = 0, J^{2f} = -0.4$ ), namely no magnetic frustration, the transition takes place at a much higher temperature  $T_c^m \simeq 1.25$ . The magnetic order parameters shown in Figure 5b confirm the skyrmion transition temperatures seen by the curvature change of the energy in Figure 5a.

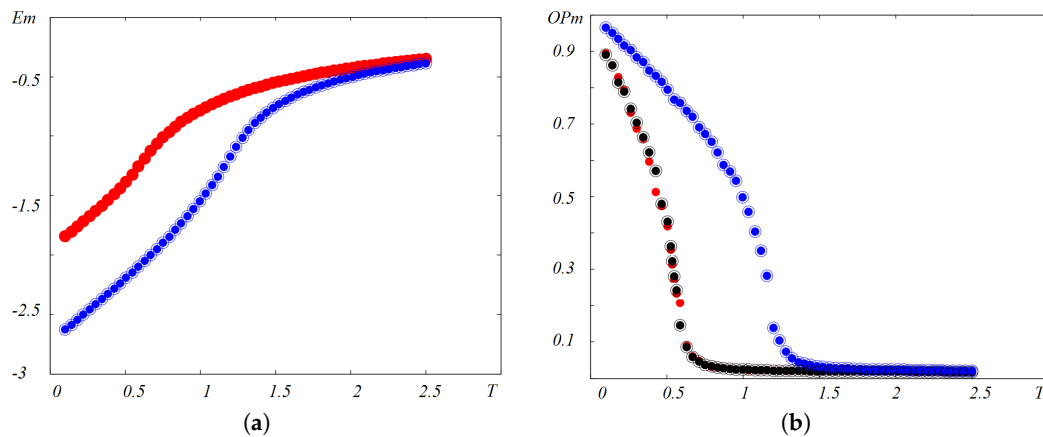


**Figure 5.** (a) Energy of the magnetic films versus temperature  $T$  for ( $J^{2m} = J^{2f} = -0.4$ ) (red), coinciding with the curve for ( $J^{2m} = -0.4, J^{2f} = 0$ ) (black, hidden behind the red curve). Blue curve is for ( $J^{2m} = 0, J^{2f} = -0.4$ ); (b) order parameter of the magnetic films versus temperature  $T$  for ( $J^{2m} = J^{2f} = -0.4$ ) (red), ( $J^{2m} = -0.4, J^{2f} = 0$ ) (black), ( $J^{2m} = 0, J^{2f} = -0.4$ ) (blue). Other used parameters:  $J^{mf} = -1.25, H = 0.25$ .

## 5. Conclusions

We have briefly shown in this paper some striking features of the properties of a magneto-ferroelectric superlattice. We have taken into account a DM interaction at the interface and the frustration due to the NNN interactions. The skyrmion crystal is shown to be stable at finite temperatures. This may have interesting applications in transport by skyrmions.

**Funding:** This research received no external funding.

**Conflicts of Interest:** The authors declare no conflict of interest.

## References

1. Bogdanov, A.N.; Yablonskii, D. Thermodynamically stable vortices in magnetically ordered crystals: The mixed state of magnets. *Zh. Eksp. Teor. Fiz* **1989**, *95*, 178.
2. Yu, X.; Onose, Y.; Kanazawa, N.; Park, J.; Han, J.; Matsui, Y.; Nagaosa, N.; Tokura, Y. Real-space observation of a two-dimensional skyrmion crystal. *Nature* **2010**, *465*, 901.
3. Yu, X.; Kanazawa, N.; Onose, Y.; Kimoto, K.; Zhang, W.; Ishiwata, S.; Matsui, Y.; Tokura, Y. Near room-temperature formation of a skyrmion crystal in thin-films of the helimagnet fege. *Nat. Mater.* **2011**, *10*, 106.
4. Heinze, S.; Bergmann, K.V.; Menzel, M.; Brede, J.; Kubetzka, A.; Wiesendanger, R.; Bihlmayer, G.; Blügel, S. Spontaneous atomic-scale magnetic skyrmion lattice in two dimensions. *Nat. Phys.* **2011**, *7*, 713.
5. Romming, N.; Hanneken, C.; Menzel, M.; Bickel, J.E.; Wolter, B.; von Bergmann, K.; Kubetzka, A.; Wiesendanger, R. Writing and deleting single magnetic skyrmions. *Science* **2013**, *341*, 636–639.
6. Rosch, A. Skyrmions: Moving with the current. *Nat. Nanotechnol.* **2013**, *8*, 160.
7. Leonov, A.; Togawa, Y.; Monchesky, T.; Bogdanov, A.; Kishine, J.; Kousaka, Y.; Miyagawa, M.; Koyama, T.; Akimitsu, J.; Koyama, T.; et al. Chiral surface twists and skyrmion stability in nanolayers of cubic helimagnets. *Phys. Rev. Lett.* **2016**, *117*, 087202.
8. Moreau-Luchaire, C.; Moutafis, C.; Reyren, N.; Sampaio, J.; Vaz, C.; Horne, N.V.; Bouzehouane, K.; Garcia, K.; Deranlot, C.; Warnicke, P.; et al. Additive interfacial chiral interaction in multilayers for stabilization of small individual skyrmions at room temperature. *Nat. Nanotechnol.* **2016**, *11*, 444.
9. Soumyanarayanan, A.; Raju, M.; Oyarce, A.G.; Tan, A.K.; Im, M.-Y.; Petrović, A.P.; Ho, P.; Khoo, K.; Tran, M.; Gan, C.; et al. Tunable room-temperature magnetic skyrmions in ir/fe/co/pt multilayers. *Nat. Mater.* **2017**, *16*, 898.
10. Dupé, B.; Bihlmayer, G.; Böttcher, M.; Blügel, S.; Heinze, S. Engineering skyrmions in transition-metal multilayers for spintronics. *Nat. Commun.* **2016**, *7*, 11779.
11. Müller, J.; Rosch, A.; Garst, M. Edge instabilities and skyrmion creation in magnetic layers. *New J. Phys.* **2016**, *18*, 065006.
12. Rosch, A. Spintronics: Electric control of skyrmions. *Nat. Nanotechnol.* **2017**, *12*, 103.
13. Shen, L.; Xia, J.; Zhao, G.; Zhang, X.; Ezawa, M.; Tretiakov, O.A.; Liu, X.; Zhou, Y. Spin torque nano-oscillators based on antiferromagnetic skyrmions. *Appl. Phys. Lett.* **2019**, *114*, 042402.
14. Fert, A.; Cros, V.; Sampaio, J. Skyrmions on the track. *Nat. Nanotechnol.* **2013**, *8*, 152.
15. Bessarab, P.; Yudin, D.; Gulevich, D.; Wadley, P.; Titov, M.; Tretiakov, O.A. Stability and lifetime of antiferromagnetic skyrmions. *Phys. Rev. B* **2019**, *99*, 140411.
16. Tomasello, R.; Martinez, E.; Zivieri, R.; Torres, L.; Carpentieri, M.; Finocchio, G. A strategy for the design of skyrmion racetrack memories. *Sci. Rep.* **2014**, *4*, 6784.
17. Koshibae, W.; Kaneko, Y.; Iwasaki, J.; Kawasaki, M.; Tokura, Y.; Nagaosa, N. Memory functions of magnetic skyrmions. *Jpn. J. Appl. Phys.* **2015**, *54*, 053001.
18. Kang, W.; Huang, Y.; Zheng, C.; Lv, W.; Lei, N.; Zhang, Y.; Zhang, X.; Zhou, Y.; Zhao, W. Voltage controlled magnetic skyrmion motion for racetrack memory. *Sci. Rep.* **2016**, *6*, 23164.
19. Zhang, X.; Xia, J.; Zhou, Y.; Liu, X.; Zhang, H.; Ezawa, M. Skyrmion dynamics in a frustrated ferromagnetic film and current-induced helicity locking-unlocking transition. *Nat. Commun.* **2017**, *8*, 1717.
20. Mühlbauer, S.; Binz, B.; Jonietz, F.; Pfleiderer, C.; Rosch, A.; Neubauer, A.; Georgii, R.; Böni, P. Skyrmion lattice in a chiral magnet. *Science* **2009**, *323*, 915–919.
21. Du, H.; Che, R.; Kong, L.; Zhao, X.; Jin, C.; Wang, C.; Yang, J.; Ning, W.; Li, R.; Jin, C.; et al. Edge-mediated skyrmion chain and its collective dynamics in a confined geometry. *Nat. Commun.* **2015**, *6*, 8504.
22. Jiang, W.; Upadhyaya, P.; Zhang, W.; Yu, G.; Jungfleisch, M.B.; Fradin, F.Y.; Pearson, J.E.; Tserkovnyak, Y.; Wang, K.L.; Heinonen, O.; et al. Blowing magnetic skyrmion bubbles. *Science* **2015**, *349*, 283–286.
23. Leonov, A.; Monchesky, T.; Romming, N.; Kubetzka, A.; Bogdanov, A.; Wiesendanger, R. The properties of isolated chiral skyrmions in thin magnetic films. *New J. Phys.* **2016**, *18*, 065003.
24. Woo, S.; Litzius, K.; Krüger, B.; Im, M.-Y.; Caretta, L.; Richter, K.; Mann, M.; Krone, A.; Reeve, R.M.; Weigand, M.; et al. Observation of room-temperature magnetic skyrmions and their current-driven dynamics in ultrathin metallic ferromagnets. *Nat. Mater.* **2016**, *15*, 501.

25. Jiang, W.; Zhang, X.; Yu, G.; Zhang, W.; Wang, X.; Jungfleisch, M.B.; Pearson, J.E.; Cheng, X.; Heinonen, O.; Wang, K.L.; et al. Direct observation of the skyrmion hall effect. *Nat. Phys.* **2017**, *13*, 162.
26. Litzius, K.; Lemesh, I.; Krüger, B.; Bassirian, P.; Caretta, L.; Richter, K.; Büttner, F.; Sato, K.; Tretiakov, O.A.; Förster, J.; et al. Skyrmion hall effect revealed by direct time-resolved X-ray microscopy. *Nat. Phys.* **2017**, *13*, 170.
27. Woo, S.; Song, K.M.; Han, H.-S.; Jung, M.-S.; Im, M.-Y.; Lee, K.-S.; Song, K.S.; Fischer, P.; Hong, J.-I.; Choi, J.W.; et al. Spin-orbit torque-driven skyrmion dynamics revealed by time-resolved X-ray microscopy. *Nat. Commun.* **2017**, *8*, 15573.
28. Seki, S.; Yu, X.; Ishiwata, S.; Tokura, Y. Observation of skyrmions in a multiferroic material. *Science* **2012**, *336*, 198–201.
29. Nahas, Y.; Prokhorenko, S.; Louis, L.; Gui, Z.; Kornev, I.; Bellaiche, L. Discovery of stable skyrmionic state in ferroelectric nanocomposites. *Nat. Commun.* **2015**, *6*, 8542.
30. Kézsmárki, I.; Bordács, S.; Milde, P.; Neuber, E.; Eng, L.; White, J.; Rønnow, H.M.; Dewhurst, C.; Mochizuki, M.; Yanai, K.; et al. Néel-type skyrmion lattice with confined orientation in the polar magnetic semiconductor  $\text{GaV}_4\text{S}_8$ . *Nat. Mater.* **2015**, *14*, 1116.
31. Hog, S.E.; Bailly-Reyre, A.; Diep, H.T. Stability and phase transition of skyrmion crystals generated by dzyaloshinskii-moriya interaction. *J. Magn. Magn. Mater.* **2018**, *455*, 32.
32. Sharafullin, I.F.; Kharrasov, M.K.; Diep, H.T. Dzyaloshinskii-moriya interaction in magnetoferroelectric superlattices: Spin waves and skyrmions. *Phys. Rev. B* **2019**, *99*, 214420.
33. Zheng, H.; Wang, J.; Lofland, S.; Ma, Z.; Mohaddes-Ardabili, L.; Zhao, T.; Salamanca-Riba, L.; Shinde, S.; Ogale, S.; Bai, F.; et al. Multiferroic  $\text{BaTiO}_3\text{-CoFe}_2\text{O}_4$  nanostructures. *Science* **2004**, *303*, 661–663.
34. Bibes, M.; Barthélémy, A. Multiferroics: Towards a magnetoelectric memory. *Nat. Mater.* **2008**, *7*, 425.
35. Sergienko, I.A.; Dagotto, E. Role of the dzyaloshinskii-moriya interaction in multiferroic perovskites. *Phys. Rev. B* **2006**, *73*, 094434.
36. Pinettes, C.; Diep, H.T. Phase transition and phase diagram of the  $j_1$ - $j_2$  heisenberg model on a simple cubic lattice. *J. Appl. Phys.* **1998**, *83*, 6317.
37. Hoang, D.-T.; Magnin, Y.; Diep, H.T. Spin resistivity in the frustrated  $j_1$ - $j_2$  model. *Mod. Phys. Lett.* **2011**, *25*, 937.
38. Yang, H.; Chen, G.; Cotta, A.A.C.; Diaye, A.T.N.; Nikolaev, S.A.; Soares, E.A.; Macedo, W.A.A.; Liu, K.; Schmid, A.K.; Fert, A.; et al. Significant dzyaloshinskii-moriya interaction at graphene-ferromagnet interfaces due to the rashba effect. *Nat. Mater.* **2018**, *17*, 605.
39. Manchon, A.; Koo, H.C.; Nitta, J.; Frolov, S.; Duine, R. New perspectives for rashba spin-orbit coupling. *Nat. Mater.* **2015**, *14*, 871.
40. Diep, H.T. Quantum theory of helimagnetic thin films. *Phys. Rev. B* **2015**, *91*, 014436.
41. Hog, S.E.; Diep, H.T.; Puzkarski, H. Theory of magnons in spin systems with Dzyaloshinskii-Moriya interaction. *J. Phys. Condens. Matter* **2017**, *29*, 305001.
42. Landau, D.P.; Binder, K. *A Guide to Monte Carlo Simulations in Statistical Physics*; Cambridge University Press: London, UK, 2009.
43. Mézard, M.; Parisi, M.; Virasoro, M. *Spin Glass Theory and Beyond An Introduction to the Replica Method and Its Applications*; World Scientific: Singapore, 1986.

